Letter

All-optical resonant magnetization switching in CrI_3 monolayers

A. Kudlis,[1,*] I. Iorsh,[1] and I. A. Shelykh[1,2,†]
[1]*Department of Physics and Engineering, ITMO University, St. Petersburg 197101, Russia*
[2]*Science Institute, University of Iceland, Dunhagi-3, IS-107 Reykjavik, Iceland*

(Received 27 April 2021; revised 12 July 2021; accepted 15 July 2021; published 27 July 2021)

Efficient control of a magnetization without an application of the external magnetic fields is the ultimate goal of spintronics. We demonstrate that in monolayers of CrI_3, magnetization can be switched all optically by application of the resonant pulses of circularly polarized light. This happens because of the efficient coupling of the lattice magnetization with a bright excitonic transition. CrI_3 is thus a perspective functional material with high potential for applications in the domains of spintronics and ultrafast magnetic memory.

DOI: 10.1103/PhysRevB.104.L020412

Introduction. The requirements of information processing demand performing at low cost, high speed, and high-density magnetic recording, without the need for the application of external magnetic fields. The achievement of this aim is among the main goals of spintronics. In conventional semiconductors, the spin of electrons can be controlled by application of the electric field via Rashba spin orbit interaction [1–3]. However, magnetic devices based on electrostatic control of individual spins have certain practical disadvantages, related to the necessity of reaching sub-Kelvin temperatures and limitations for characteristic times of the spin inversion. Therefore, the search for novel magnetic materials and devices which reveal efficient and controllable magnetization switching continues.

The possibility of an optical control of magnetization is of special interest here, as it can potentially push the speed of the magnetic reversal and associated magnetic memory writing speed towards THz frequencies. Optical magnetization switching was very recently demonstrated for CdFeCo [4–8] and TbFeCo [9] ferromagnetic alloys, as well as in Co/Gd bilayers [10].

In this context, the family of functional two-dimensional (2D) materials, namely, chromium dichalcogenides, such as CrI_3 and $CrBr_3$, is of special interest, as they possess a unique combination of optical and magnetic properties. In particular, they demonstrate a robust optical excitonic response, with record high values of excitonic binding energies and oscillator strengths [11], exceeding even the values reported for transition metal dichalcogenides [12–15]. At the same time, these materials are 2D Ising ferromagnets [16–18], thus having an additional twist related to the giant Zeeman splitting of the valence and conduction bands, which, among others, strongly affects their optical properties, leading to such phenomena as the giant Kerr response [16], magnetic circular dichroism [19], and onset of 2D magnetoplasmons [20].

In this Letter, we demonstrate that the combination of the pronounced excitonic and ferromagnetic responses leads to the possibility of polarization selective switching of the magnetization. The main idea of the proposed effect is illustrated schematically in Fig. 1. The band structure of a monolayer of CrI_3 is shown schematically in Fig. 1 (lower panel). As CrI_3 is a direct band semiconductor, the optical transition is allowed from the top of the valence band to the bottom of the conduction band. Attraction between an electron and a hole leads to the formation of strongly coupled bright excitons. Depending on the direction of the magnetization of a sample, ground-state excitons can be excited by σ^+ or σ^- light.

Consider the geometry shown in the lower panel of Fig. 1, when the ground state corresponds to σ^- excitation and we send a pulse of σ^+ light in resonance with it. As the σ^+ transition is strongly offset in energy due to the giant Zeeman splitting produced by the lattice magnetization, the absorption of σ^+ photons is only virtual. However, this virtual absorption creates an effective magnetic field, which tends to invert the magnetization. This process is favored by the fact that the magnetization switch will make optical absorption resonant, and if the intensity of the optical pump exceeds some threshold value, it finally happens.

Methods. To describe the process of magnetization switching, we proposed a phenomenological model based on the system of coupled driven-dissipative Gross-Pitaevskii-type equations for the concentration of spin polarized excitons with a Landau-Lifshitz-Gilbert equation for the lattice magnetization. It is worth noting that taking phonons into account in systems of this type can notably change the quantitative picture. However, in our work, we considered the most basic model to demonstrate the mechanism of exciton-assisted magnetization switching.

The total effective magnetic field affecting the dynamics of the magnetization can be estimated as the sum of a real magnetic field $\boldsymbol{H}_0$, magnetic field provided by spin-spin interactions $\boldsymbol{H}_{\text{ex}}$, and an effect provided by spin polarized excitons,

$$\boldsymbol{H} = \boldsymbol{H}_0 + \boldsymbol{H}_{\text{ex}} + \delta(|\psi_+|^2 - |\psi_-|^2)\boldsymbol{e}_z, \tag{1}$$

*andrew.kudlis@metalab.ifmo.ru
†shelykh@hi.is

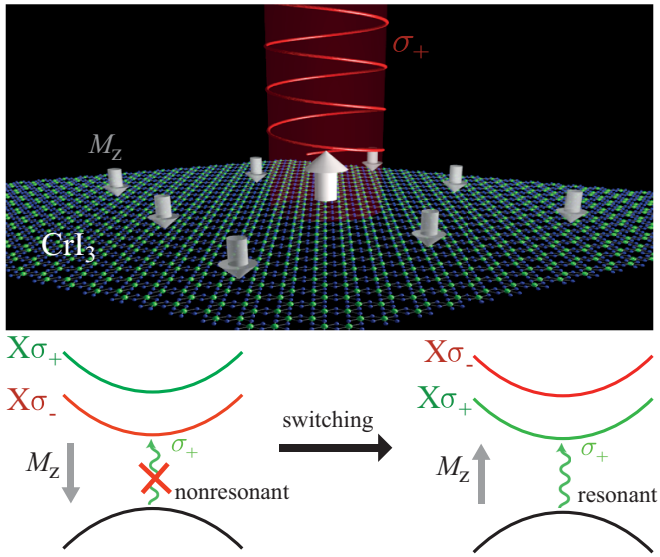

FIG. 1. Upper panel: A monolayer of CrI_3 is irradiated by a circularly polarized light which reverses its magnetization. Lower panel: The mechanism of the magnetization switching. The circular polarized pump is not resonant with the corresponding exciton transition if magnetization is pointing down (left part), but becomes resonant if the direction of the magnetization is switched.

where ψ_+ and ψ_- are order parameters which correspond to the densities of excitons with spin up and spin down, respectively, $n_\pm = |\psi_\pm|^2$, and

$$\boldsymbol{H}_{\rm ex} = A\,\nabla^2\boldsymbol{M} + D\,\nabla\times\boldsymbol{M}, \tag{2}$$

where the constants A and D characterize the exchange interaction of the Heisenberg and Dzyaloshinskii-Moriya type, respectively [21]. It is easy to also note that the natural choice of the combination $|\psi_+|^2 - |\psi_-|^2$ for the average spin density allows one to preserve the time-reversal symmetry in the corresponding effective energy functional.

This effective field enters into the Landau-Lifshitz equation describing the magnetization dynamics [21,22],

$$\frac{\partial \boldsymbol{M}}{\partial t} = -\gamma[\boldsymbol{M}\times\boldsymbol{H}] - \frac{\gamma\eta}{M_s}[\boldsymbol{M}\times[\boldsymbol{M}\times\boldsymbol{H}]], \tag{3}$$

where $\boldsymbol{M}$ is magnetization, M_s is its saturation value, $\gamma = \mu_0\gamma_0$, $\gamma_0 = g\mu_B/\hbar$, and η is a dimensionless damping constant. To close the system of the equations, one also needs to write the equations for the dynamics of the excitonic fields, which in the simplest case can be chosen in the form of the driven-dissipative Gross-Pitaevskii equations for the components ψ_+ and ψ_- [23,24],

$$i\hbar\frac{\partial\psi_+}{\partial t} = -\frac{\hbar^2}{2m_X}\nabla^2\psi_+ + \beta M_z\psi_+ + \alpha|\psi_+|^2\psi_+ + P_+e^{i\delta_+ t}, \tag{4}$$

$$i\hbar\frac{\partial\psi_-}{\partial t} = -\frac{\hbar^2}{2m_X}\nabla^2\psi_+ - \beta M_z\psi_- + \alpha|\psi_-|^2\psi_- + P_-e^{i\delta_- t}, \tag{5}$$

where m_X is the exciton mass, and P_+ and P_- are the pump amplitudes in the right and left circularly polarized components, respectively. They are related to the corresponding pump power densities $W_\pm$ as follows: $W_\pm = P_\pm^2\omega_{\rm ex}/\hbar f_0$, where $\omega_{\rm ex}$ is the exciton frequency and f_0 is its oscillator strength. The coupling constants δ and β are related to each other, as both of them describe the mutual action of the excitonic and magnetic subsystems. To estimate the corresponding relation, one can assume that the maximum of the product βM_s, corresponding to the Zeeman splitting of the excitons, should be approximately equal to the characteristic energy $\hbar\gamma H$ entering into Landau-Lifshitz equation for the case when the concentration of polarized excitons is around one per unit cell of size $d\times d$:

$$\hbar\gamma\delta/d^2 \approx \beta M_s. \tag{6}$$

In our analysis, we consider the case of the spatially homogeneous optical pump and suggest that both $\boldsymbol{M}$ and $\psi_\pm$ do not have any spatial dependence. This will allow us to drop the term related to the exchange interaction in the expression for the effective magnetic field [Eq. (2)]. Moreover, we can introduce the following set of dimensionless variables:

$$\tilde{\boldsymbol{M}} = \frac{\boldsymbol{M}}{M_s},\quad \tilde\psi_\pm = \frac{\psi_\pm}{\psi_s},\quad \tilde t = \frac{t}{t_s},\quad \tilde P_\pm = \frac{P_\pm}{P_s},$$
$$\tilde W_\pm = \frac{W_\pm}{W_s},\quad \tilde{\boldsymbol{H}}_0 = \frac{\boldsymbol{H}_0}{M_s},\quad \tilde{\boldsymbol{H}} = \frac{\boldsymbol{H}}{M_s}.$$

This will allow us to rewrite the system of the dynamic equations in the following form:

$$\tilde{\boldsymbol{H}} = \tilde{\boldsymbol{H}}_0 + (|\tilde\psi_+|^2 - |\tilde\psi_-|^2)\boldsymbol{e}_z, \tag{7}$$

$$\frac{d\tilde{\boldsymbol{M}}}{d\tilde t} = -[\tilde{\boldsymbol{M}}\times\tilde{\boldsymbol{H}}] - \eta[\tilde{\boldsymbol{M}}\times[\tilde{\boldsymbol{M}}\times\tilde{\boldsymbol{H}}]], \tag{8}$$

$$i\frac{d\tilde\psi_+}{d\tilde t} = a_1\tilde M_z\tilde\psi_+ + a_2|\tilde\psi_+|^2\tilde\psi_+ + \tilde P_+e^{i\tilde\delta_+\tilde t}, \tag{9}$$

$$i\frac{d\tilde\psi_-}{d\tilde t} = -a_1\tilde M_z\tilde\psi_- + a_2|\tilde\psi_-|^2\tilde\psi_- + \tilde P_-e^{i\tilde\delta_-\tilde t}, \tag{10}$$

where the corresponding dimensionless parameters expressed in terms of the original ones are given in Table I. As for the numerical values of the parameters, we use the following numbers. The value of exciton frequency $\hbar\omega_{\rm ex}$ is chosen as 1.5 eV [16,25], while $\hbar f_0$ is assumed to equal to 0.033 eV. The value of the saturation magnetization for CrI_3 is chosen as $M_s = 0.137$ mA/layer [26]. The constant α responsible for the nonlinearity is expected to be the same as for the excitons in transition metal dichalcogenide monolayers [27], and is taken as 0.1 eV $\times$ 1 nm^2. The estimation of δ is done using the relation (6) with $\beta M_s = 0.06$ eV. The characteristic size of unit cell d is assumed to be 1 nm. This parameter implicitly defines the threshold power required for switching. Also, due to the fact that d enters the equations quadratically, the theory is noticeably sensitive to its variations. We associate this quantity with the unit cell size and take the typical number; however, the exact value for CrI_3 may deviate from this simple estimation, which would affect the value of the threshold power. The determination of the Gilbert damping constant is a serious computational challenge and deserves a

TABLE I. Definitions of parameters which enter the system of Eqs. (7)–(10). The quantities designed to make the variables dimensionless are also presented. The corresponding numerical values are calculated on the basis of numbers for M_s, δ, d, ω_{ex}, f_0, and α discussed within the body of the text.

Parameter	Definition	Value	Parameter	Definition	Value
a_1	$\delta/d^2 M_s$	2134	t_s	$1/\gamma M_s$	2.33×10^{-2} ns
a_2	$\alpha/\delta\gamma\hbar$	1.663	ψ_s	$\sqrt{M_s/\delta}$	2.16×10^{5} cm^{-1}
$\tilde{\delta}_+$	$\delta_\pm t_s$	11.04	P_s	$\psi_s\hbar/t_s$	9.77×10^{-17} J cm^{-1}
$\tilde{\delta}_-$	$\delta_\pm t_s$	0.000	W_s	$P_s^2\omega_{ex}/\hbar f_0$	4.12×10^{-1} W cm^{-2}

separate consideration; however, the typical values for such layer materials are expected to be measured within the following range: $\eta \in [0.01, 0.1]$ [28]. We would like to stress that although our choice of the parameters is typical for 2D materials, their exact values for the considered material cannot be defined with any satisfactory precision at the current stage of knowledge.

Results and discussion. Based on Eqs. (7)–(10), the dynamics of the system is analyzed. The typical behavior of magnetization $\tilde{\boldsymbol{M}}$ and density $|\tilde{\psi}_+|^2$ is shown in Fig. 2. The initial state corresponds to no excitons present in the system and magnetization pointing down. As one can see, after characteristic transition time $\tilde{\tau}$, the direction of the magnetization switches and the excitonic concentration increases in a steplike manner, as the condition of the resonant absorption is achieved. In the same time, in-plane components of the magnetization exhibit oscillations in the transient regime, but remain zero after the switching.

The main parameter characterizing the switching is the transition time $\tilde{\tau}$. Its dependence on the pump power density $\tilde{W}_+$ for the case when $\tilde{\boldsymbol{H}}_0 = 0$ for various values of the damping parameter η is shown in Fig. 3. Naturally, $\tilde{\tau}$ decreases with an increase of $\tilde{W}_+$, and the corresponding dependence can be perfectly fitted by the following phenomenological relation:

$$\tilde{\tau} = \frac{b}{\eta \tilde{W}_+}. \tag{11}$$

For the set of parameters corresponding to Table I, nanosecond switching times are reached for the pump intensities of about 10^5 W cm^2. Note that in the simple model we use, where the processes of the excitonic decoherence are neglected, there is no threshold for the magnetization switching in the case when the external z-directed magnetic field is absent.

The application of the external magnetic field $\tilde{\boldsymbol{H}}_0$ strongly affects the switching process. The application of the lateral field leads to the rapid decrease of $\tilde{\tau}$ as can be seen in Fig. 4. This effect has a clear physical meaning, as the in-plane field produces additional torque acting on the z component of the magnetization. In contrast to the case when $\tilde{\boldsymbol{H}}_0$ is zero, here we do not find a simple fit for $\tilde{\tau}$ on the whole field range. However, in the regime when the external field is small ($\tilde{H}_x \ll 1$), the following approximation is valid:

$$\tilde{\tau} = \frac{b}{\eta \tilde{W}_+ (1 + a\tilde{H}_x)^\kappa}, \tag{12}$$

where the parameters a and κ are estimated as 120 and 0.4, respectively. We did not manage to get a simple universal relation describing the behavior of $\tilde{\tau}$ in the region of big strong

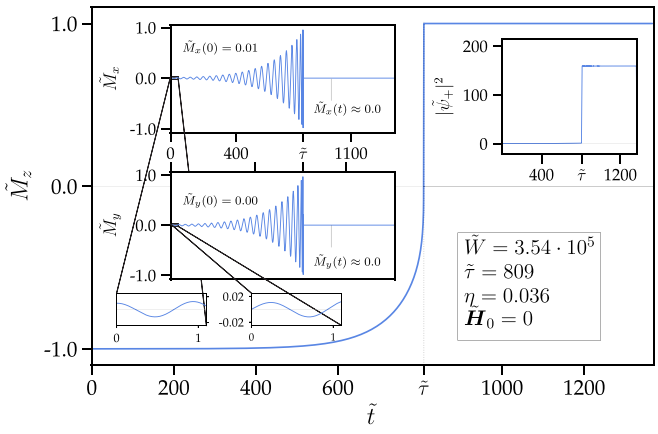

FIG. 2. Dependencies of magnetization components $\tilde{M}_x$, $\tilde{M}_y$, and $\tilde{M}_z$ as well as the density $|\tilde{\psi}_+|^2$ on time obtained by solving Eqs. (7)–(10) in the case of the absence of the external magnetic field ($\tilde{\boldsymbol{H}}_0 = 0$). The transition time is denoted by $\tilde{\tau}$. The initial state corresponds to no excitons present in the system and magnetization pointing down. After a characteristic transition time, the direction of the magnetization switches and the excitonic concentration increases in a steplike manner. In plane, the components exhibit oscillations in the transient regime, but are zero after the switching.

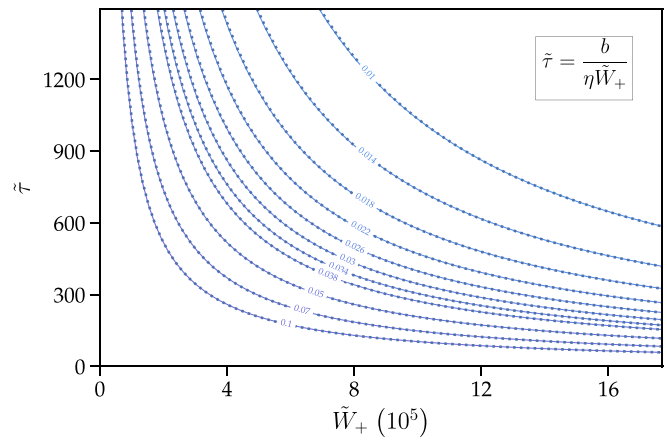

FIG. 3. The dependence of the transition time $\tilde{\tau}$ on the power density of the circularly polarized pump $\tilde{W}_+$ for different values of Gilbert damping constant η for the case of the absence of the external magnetic field, $\tilde{\boldsymbol{H}}_0 = 0$. All the curves were fitted by expression (11) (dotted lines), which gives the perfect match for $b = 1.04 \times 10^7$.

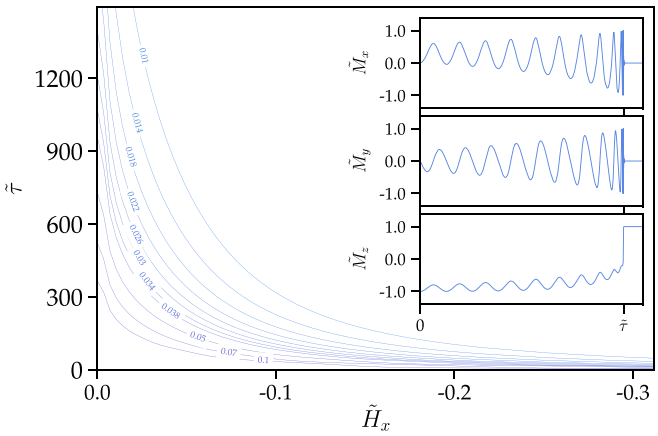

FIG. 4. The dependence of the transition time $\tilde{\tau}$ on the lateral external magnetic field ($\tilde{\boldsymbol{H}}_0 = \tilde{H}_x \vec{e}_x$) for different values of Gilbert damping constant η at fixed value of the intensity of the circularly polarized pump ($\tilde{W}_+ = 2.83 \times 10^5$). As one can see, the lateral field favors the switching, reducing the corresponding characteristic time.

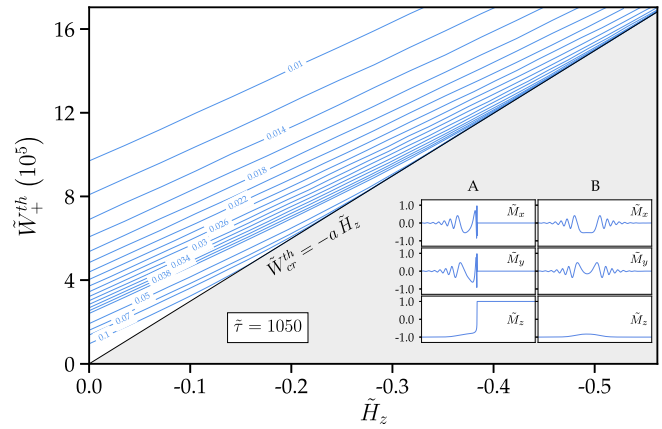

FIG. 5. Effect of the application of the external z-directed magnetic field $\tilde{\boldsymbol{H}}_0 = \boldsymbol{e}_z \tilde{H}_z$ on polarization switching. The gray region corresponds to the regime when switching does not occur at any time. The threshold intensity is well described by the dependencies of the threshold value, $\tilde{W}_+^{\text{th}} = aH_z$. In the white region, the blue curves correspond to constant values of the switching time $\tilde{\tau} = 1050$ for different values of η. It is seen that bigger intensities are needed to keep the switching time constant with increase of H_z and therefore the perpendicular magnetic field is not favorable for the switching. The insets show the temporal dependence of the components of the magnetization switching, when the intensity of the pump is above the threshold (panels A) and below it (panels B) for the case $\eta = 0.1$.

lateral magnetic fields, but it decays faster than in expression (12). For the choice of the parameters that we use, the lateral field of 1 T will lead to the decrease of the switching time by 10^3, which will allow one to reduce the values of the pump needed to reach the nanosecond switching times by the same factor.

The case when the external magnetic field is applied along the z axis is illustrated in Fig. 5. In contrast to the cases of absent and lateral external fields, here the threshold for the magnetization switching appears. The threshold intensity linearly increases with the increase of $\tilde{H}_z$, and if the pump is below the threshold, the switching does not occur at any time (gray region in the plot). Above the threshold, the increase of the z-directed external field leads to the decrease of the switching time, as can be seen from the blue curves, corresponding to constant values of $\tilde{\tau}$. Thus, in general, contrary to the case of the lateral field, the z-directed magnetic field is not favorable for the switching. Finally, it is clear that relatively large threshold intensities would inevitably lead to sample heating, which, in turn, can lead to the magnetization switching at the subnanosecond (for ferromagnets) and picosecond (for antiferromagnets) timescales [29]? The exciton-assisted mechanism can be easily discriminated from the heating induced by the resonant dependence on the pulse central frequency.

Conclusions. In conclusion, we developed a phenomenological theory of all optical resonant magnetization control in CrI_3 monolayers. It was demonstrated that the presence of the robust bright excitonic resonances coupled to lattice magnetization leads to the possibility of polarization-sensitive magnetization switching in the nonlinear regime. We investigated the dependence of the switching time on pump intensity and external magnetic field, demonstrating that lateral fields are favorable for the switching, reducing the switching time, while perpendicular fields have the opposite effect. Our results can be used for the practical development of ultrafast magnetic memory elements.

Acknowledgements. The work was funded by RFBR and DFG, Project No. 21-52-12038. I.A.S. acknowledges support from the Icelandic Research Fund (project "Hybrid polaritonics"). The authors also acknowledge funding from the Ministry of Education and Science of the Russian Federation through Megagrant (Project 075-15-2021-589).

[1] S. Datta and B. Das, Appl. Phys. Lett. **56**, 665 (1990).
[2] S. D. Ganichev, V. V. Belkov, L. E. Golub, E. L. Ivchenko, P. Schneider, S. Giglberger, J. Eroms, J. De Boeck, G. Borghs, W. Wegscheider, D. Weiss, and W. Prettl, Phys. Rev. Lett. **92**, 256601 (2004).
[3] H. C. Koo, J. H. Kwon, J. Eom, J. Chang, S. H. Han, and M. Johnson, Science **325**, 1515 (2009).
[4] D. O. Ignatyeva, C. S. Davies, D. A. Sylgacheva, A. Tsukamoto, H. Yoshikawa, P. O. Kapralov, A. Kirilyuk, V. I. Belotelov, and A. V. Kimel, Nat. Commun. **10**, 4786 (2019).
[5] L. Aviles-Flix, A. Olivier, G. Li, C. S. Davies, L. Alvaro-Gomez, M. Rubio-Roy, S. Auffret, A. Kirilyuk, A. V. Kimel, T. Rasing, L. D. Buda-Prejbeanu, R. C. Sousa, B. Dieny, and I. L. Prejbeanu, Sci. Rep. **10**, 5211 (2020).
[6] C. D. Stanciu, F. Hansteen, A. V. Kimel, A. Kirilyuk, A. Tsukamoto, A. Itoh, and T. Rasing, Phys. Rev. Lett. **99**, 047601 (2007).
[7] C. S. Davies, T. Janssen, J. H. Mentink, A. Tsukamoto, A. V. Kimel, A. F. G. van der Meer, A. Stupakiewicz, and A. Kirilyuk, Phys. Rev. Appl. **13**, 024064 (2020).

[8] J. Igarashi, Q. Remy, S. Iihama, G. Malinowski, M. Hehn, J. Gorchon, J. Hohlfeld, S. Fukami, H. Ohno, and S. Mangin, Nano Lett. **20**, 8654 (2020).
[9] X. Lu, X. Zou, D. Hinzke, T. Liu, Y. Wang, T. Cheng, J. Wu, T. A. Ostler, J. Cai, U. Nowak, R. W. Chantrell, Y. Zhai, and Y. Xu, Appl. Phys. Lett. **113**, 032405 (2018).
[10] Y. L. W. van Hees, P. van de Meugheuvel, B. Koopmans, and R. Lavrijsen, Nat. Commun. **11**, 3835 (2020).
[11] M. Wu, Z. Li, T. Cao, and S. G. Louie, Nat. Commun. **10**, 2371 (2019).
[12] A. Chernikov, T. C. Berkelbach, H. M. Hill, A. Rigosi, Y. Li, O. B. Aslan, D. R. Reichman, M. S. Hybertsen, and T. F. Heinz, Phys. Rev. Lett. **113**, 076802 (2014).
[13] A. Splendiani, L. Sun, Y. Zhang, T. Li, J. Kim, C.-Y. Chim, G. Galli, and F. Wang, Nano Lett. **10**, 1271 (2010).
[14] P. Steinleitner, P. Merkl, P. Nagler, J. Mornhinweg, C. Schüller, T. Korn, A. Chernikov, and R. Huber, Nano Lett. **17**, 1455 (2017).
[15] G. Wang, A. Chernikov, M. M. Glazov, T. F. Heinz, X. Marie, T. Amand, and B. Urbaszek, Rev. Mod. Phys. **90**, 021001 (2018).
[16] B. Huang, G. Clark, E. Navarro-Moratalla, D. R. Klein, R. Cheng, K. L. Seyler, D. Zhong, E. Schmidgall, M. A. McGuire, W. Cobden, D. H. Yao, D. Xiao, P. Jarillo-Herrero, and X. Xu, Nature (London) **546**, 270 (2017).
[17] F. Zheng, J. Zhao, Z. Liu, M. Li, M. Zhou, S. Zhang, and P. Zhang, Nanoscale **10**, 14298 (2018).
[18] I. V. Kashin, V. V. Mazurenko, M. I. Katsnelson, and A. N. Rudenko, 2D Mater. **7**, 025036 (2020).
[19] K. L. Seyler, D. Zhong, D. R. Klein, S. Gao, X. Zhang, B. Huang, E. Navarro-Moratalla, L. Yang, D. H. Cobden, M. A. McGuire, W. Yao, D. Xiao, P. Jarillo-Herrero, and X. Xu, Nat. Phys. **14**, 277 (2018).
[20] A. A. Pervishko, D. Yudin, V. K. Gudelli, A. Delin, O. Eriksson, and G.-Y. Guo, Opt. Express **28**, 29155 (2020).
[21] C. Abert, Eur. Phys. J. B **92**, 120 (2019).
[22] J. Leliaert and J. Mulkers, J. Appl. Phys. **125**, 180901 (2019).
[23] A. A. High, A. T. Hammack, J. R. Leonard, S. Yang, L. V. Butov, T. Ostatnický, M. Vladimirova, A. V. Kavokin, T. C. H. Liew, K. L. Campman, and A. C. Gossard, Phys. Rev. Lett. **110**, 246403 (2013).
[24] D. V. Vishnevsky, H. Flayac, A. V. Nalitov, D. D. Solnyshkov, N. A. Gippius, and G. Malpuech, Phys. Rev. Lett. **110**, 246404 (2013).
[25] A. Molina-Sánchez, G. Catarina, D. Sangalli, and J. Fernández-Rossier, J. Mater. Chem. C **8**, 8856 (2020).
[26] S. Jiang, L. Li, Z. Wang, K. F. Mak, and J. Shan, Nat. Nanotechnol. **13**, 549 (2018).
[27] V. Shahnazaryan, I. Iorsh, I. A. Shelykh, and O. Kyriienko, Phys. Rev. B **96**, 115409 (2017).
[28] K. Dolui, M. D. Petrović, K. Zollner, P. Plecháč, J. Fabian, and B. K. Nikolić, Nano Lett. **20**, 2288 (2020).
[29] A. V. Kimel, A. Kirilyuk, A. Tsvetkov, R. V. Pisarev, and Th. Rasing, Nature **429**, 850 (2004).